NEW DESIGN OF THE SFC CENTRAL REGION

J.Y. Tang, X.Q. Zhao
Institute of Modern Physics, P.O. Box 31, Lanzhou 730000, P.R. China

Abstract: The old central region of SFC has the problem of orbit centralization due to the low RF voltage. Also the same constant orbit parameters are not good for both H=1 and H=3 acceleration modes. A new central region has been studied and installed, which uses two different spiral inflectors, respectively working at H=1 mode, R_{inj}=2.5 cm, and at H=3 mode, R_{inj}=3.0 cm. The larger injection radius at H=3 mode increases the extraction voltage of the ECR ion source by 44%, and gives higher extracted beam intensity and better transmission efficiency through the injection line due to weakened space charge effect for both transversal and longitudinal phase spaces. In order to solve the low RF voltage problem, we use the constant orbit modes with small range of variation, and it keeps the orbit well centralized.

1. Introduction

In 1992, the injector cyclotron SFC of HIRFL was upgraded by replacing the internal PIG ion source with ECR ion source[1,2]. The ion source with the axial injection line and the central region has been operating but with some unsatisfactory. The main problems come from the buncher system and the injection mode. The former one is redesigned and described in Ref. 3, This paper is concentrated on the latter one. In the past, we used the same injection radius ρ_0=2.5 cm for both H=1 and H=3 harmonic acceleration modes. But the experience and the calculations show that the space charge effect is too important for H=3 mode, especially when lower Z/A ions are accelerated, due to very low injection voltage or extraction voltage for the ion source ($V_{inj} = \frac{1}{2}\frac{q}{m}(B\rho_0)^2$). The low injection voltage also means low beam intensity extracted from the ion source or bigger beam emittance for the same intensity. The new central region uses two injection radius ρ_0=2.5 cm and ρ_0=3.0 cm for H=1 and H=3 modes respectively, so the injection voltage for H=3 is increased to 1.44 time of the past value. But we need two spiral inflectors with different parameters. The electrodes of the central region has been designed to fit the two modes. The new central region also solves the problem of the beam centralization due to low maximum RF voltage. With the new injection mode, SFC harmonic acceleration diagram is showed in Fig. 1.

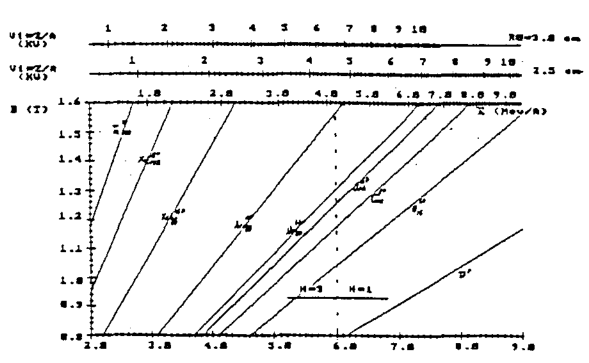

Fig. 1 SFC harmonic acceleration diagram

2. Design of the electrodes and computation of the electric field

It is some difficult to define the geometry of the electrodes which is judged well for the two modes. For the given one, we use RELAX3D program to compute the electric field map, then calculate the particle trajectory to check if it is well designed to make the orbits well centralized for the two modes. We made several times of modifications to get a satisfactory geometry. Together with the puller electrodes, the shieldings of the inflectors are also specially shaped, in order to increase the acceleration efficiency at the first two gaps. The final geometry with the calculated electric equipotential lines are shown in Fig. 2a and Fig. 2b, for H=1 and H=3 respectively. Due to the use of the nonfixed orbit, we take only one puller post, instead we use the decreased gap height (from 40 mm to 30 mm) in the first turns to make the electric field less penetrated into the Dees, therefor better transit time factor. But the phase selection by puller post is sacrified here.

3. Spiral inflectors

We keep the old spiral inflector in use for H=1 mode, but with different shielding house. For H=3 mode, a new spiral inflector has to be manufactured. The main parameters of the two inflectors are given in Table 1.

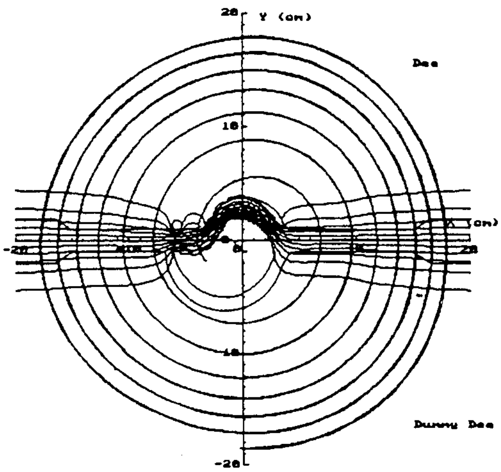

Fig.2a Central region geometry with the equipotential lines

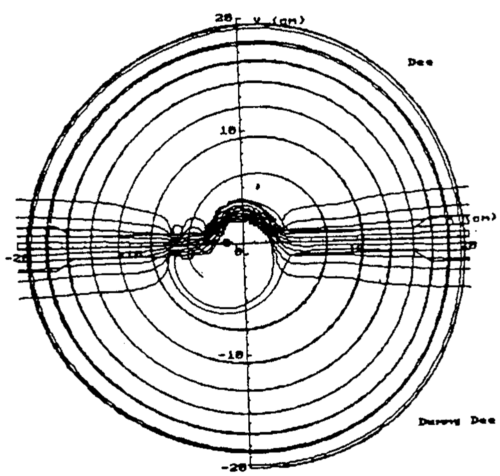

If we take the central region coordinates, the inflector for H=1 mode is rotated -10° with z-axis, but no rotation for H=3 mode. The central trajectories and curvature centres at the exits of the inflectors are:

(1) H=1, $\theta=\pi/2$, $x_e=-3.147$ cm, $y_e=-1.883$ cm, $z_e=0$, $x_{oe}=-1.619$ cm, $y_{oe}=-0.146$, $\phi_{RF}=-45°$;

(2) H=3, $\theta=\pi/2$, $x_e=-3.046$ cm, $y_e=-2.936$ cm, $z_e=0$, $x_{oe}=-1.888$ cm, $y_{oe}=-0.510$, $\phi_{RF}=-185°$.

These conditions are used as the start conditions for the trajectory calculations in the central region. We use also RELAX3D program to compute the electric field in the inflectors, in order to calculate the transfer matrix by tracing method and also to eliminate the influence of the edge effect. Both inflectors are cut off 2~3 mm at the entrance and at the exit.

Table 1, Parameters of the spiral inflector

Mode	H=1	H=3
Magnetic radius ρ_0	2.5 cm	3.0 cm
Electric radius or height A	6.0 cm	7.2 cm
K value ($K=A/\rho_0$)	2.4	2.4
Gap distance d	0.8 cm	1.0 cm
Rotation angle φ	-10°	0°
Max. voltage (V_{inj}=25 kV)	6.67 kV	6.94 kV

4. Orbit calculations

4.1) Horizontal motion

We use two methods for the trajectory calculations, ACCORB and CENTOR for the codes. The first one utilizes directly the equipotential lines, the original idea was from P. Mandrillon[6] and the code was developped by Tang at MEDICYC, Nice, France and at IMP. The similar method has been used also by J.P. Shapira[7]. It calculates the particle's motion between the equipotential lines and gives the energy gain and the curvature centre movement of the particle when crossing these lines. So it gives rather intuitive view on the acceleration pass at first gaps, and is very useful at the early stage of designing the central region geometry. The code CENTOR is the adaptation of CENTOM version at GANIL, as other widely used codes it integrates differential equations in cylindrical coordinates. It takes the bidimensional electric potential map calculated by RELAX3D.

Due to the limitation of the maximum RF voltage $V_{Dmax} \le 75$ kV, we introduce the constant orbit acceleration mode[4,5,6] with small variation, that means that the nominated modes are constant orbit accelerations, but the applied RF voltage can be lowered when the nominated voltage can not be met. In order to do so, the barycentres of the nominated orbits are designed to shift some to the positive x-coordinate as the one of the orbit with maximum variation is situated some on the negative x-coordinate. So for all the cases, the barycentre of the central trajectory is around the machine centre. Here we use injection radius ρ_0 and the increment of the curvature radius at the first gap $\Delta\rho$ to define the constant orbit acceleration mode, $\Delta\rho$ varies in a small range. The RF voltage can be got by

$$V_D = \frac{V_{inj}}{T_1}\left(2+\frac{\Delta\rho}{\rho_0}\right)\frac{\Delta\rho}{\rho_0}\ ,$$

T_1 is the transit time factor at the first gap. For the two modes, the orbit parametres are shown in Table 2.

The disadvantage for unfixed orbit acceleration is that the total acceleration turn number is not fixed and gives some problem for the beam extraction. But nevertheless we use preccessional single turn extraction which is done most by experience.

Table 2 The settings of central rays in the central region

mode	H=1	H=3
injection radius ρ_0	2.5 cm	3.0 cm
variation range $\Delta\rho$	2.355~2.925	2.402~3.036
transit time factor T_l	0.92	0.79~0.82
total accel. turns	148~110	157~120
Max. Dee voltage	75 kV	74 kV
barycentre at 7th turn	X_c=0.176 cm Y_c=-0.075 cm	X_c=0.189 cm Y_c=0.040 cm

4.2) Vertical motion

We use a cone magnetic field together with the electric field to assure the vertical focusing. The magnetic field slope begins to act after the first gap acceleration at about R=3.0 cm, and creates rather moderate focusing by using 50~100 Gauss cone field in the central region. In order to get efficient electric focusing in the vertical plane, the gap height is decreased in the first 3 turns. Also the small opening of the exit on the inflector house and the pillars on the exit side of the first gap give relatively strong vertical focusing.

For the numerical calculations, we can calculate the vertical component of the electric field from the bidimensional potential map like:

$$E_z = z\left(\frac{\partial^2 V(x,y,0)}{\partial x^2} + \frac{\partial^2 V(x,y,0)}{\partial y^2}\right)$$

or by difference quotients:

$$E_z = \frac{z}{h^2}(V(x+h,y,0)+V(x-h,y,0)+ V(x,y+h,0)+V(x,y-h,0)-4V(x,y,0))$$

where h is the mesh step.

5. Phase space acceptances

We define the radial and longitudinal acceptances as following way. At first, the reference orbit should has its barycentre close to cyclotron centre after some turns acceleration, namely it situates well inside the radial stable region. Here it is less than 3mm after 7 turns. Then the acceptance is defined by the barycentre within ±2mm from reference's one and certainly inside the radial stable region. We see the radial stable region at R=200mm or about 7th turn in Fig. 3. The calculated radial acceptances related to RF phase are shown in Fig.4. The shift of angular divergence related to the RF phase can be explained by the central position phase[8].

The vertical acceptance is easily defined by the Dee electrode gap height, and is shown in Fig. 5.

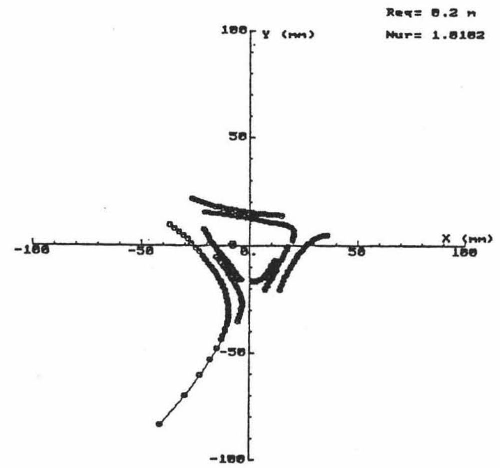

Fig. 3 Radial stable region (H=1, $^{16}O^{6+}$ 6.4 Mev/u)

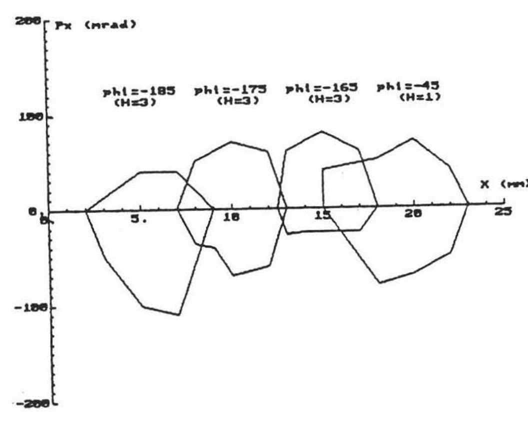

Fig. 4 Radial phase space acceptance

6. Conclusion

The new design of the central region used the constant acceleration orbit mode with small variation. It solves the problems of low RF voltage range and of the contradiction between the orbit centralization and the minimum acceleration turns. So we can use the maximum got Dee voltage at most cases without losing beam centralization. By increasing the injection voltage for H=3 mode, the space charge effect on the injection line can be weakened, at the same time the injection radius has to be increased from R_{inj}=2.5 cm to R_{inj}=3.0 cm. The new designed central region is just fitted for the two modes. Both radial and vertical motions are studied, and the admittances are acceptable.

Thanks professors Y.F. Wang, Z.R. Ma, B.W. Wei, Q.M. Yin, Q.W. Qiao, A. Chabert for their discussions and encouragement.

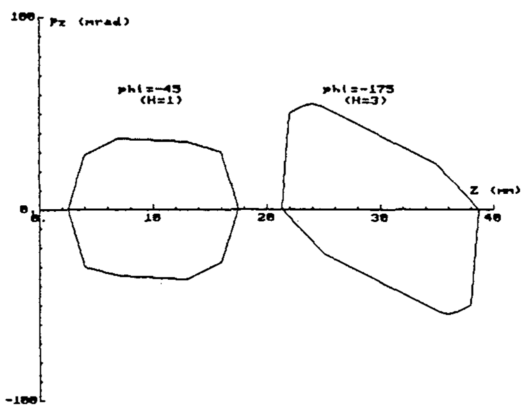

Fig. 5 Vertical phase space acceptance

Reference

1). F. Ye et al., 13th International Conference on Cyclotrons and Their Applications, Vancouver (1992) 78
2) Z.R. Ma, HIRFL Progress Report, Vol. 9 (1991)
3) J.Y. Tang, W. Lei and Y.F. Wang, this conference
4) M. Reiser, Nucl. Instr. and Meth. 18-19 (1962) 370
5) H. G. Blosser, IEEE Trans. Nucl. Sci. NS-13 (1966) 1
6) G. Bellomo, 12th International Conference on Cyclotrons and thier Applications, Berlin, (1990) 325
7) P. Mandrillon, Report IPN0-GTA/85-01, Orsay, France
8) J.P. Shapira, 10th International Conference on Cylotrons and their Applications, East Lansing, (1984) 332
9) W.M. Shulte - EUT Thesis, Eihhoven (1978)
W.M. Shulte and H.L. Hagedoorn, IEEE Trans. Nucl. Sci. NS-26 (1979) 2329
W.M. Shulte and H.L. Hagedoorn, IEEE Trans. Nucl. Sci. NS-26 (1979) 2388